

Extended finite element simulation of crack propagation in cracked Brazilian disc

M. Eftekhari*, A. Baghbanan and H. Hashemolhosseini

Department of Mining Engineering, Isfahan University of Technology, Isfahan, Iran

Received 19 May 2014; received in revised form 12 February 2015; accepted 22 February 2015

*Corresponding author: eftekhari_mosleh@yahoo.com (M. Eftekhari).

Abstract

The cracked Brazilian disc (CBD) specimen is widely used in order to determine mode-I/II and mixed-mode fracture toughness of a rock medium. In this study, the stress intensity factor (SIF) on the crack-tip in this specimen is calculated for various geometrical crack conditions using the extended-finite element method (X-FEM). This method is based upon the finite element method (FEM). In this method, the crack is modeled independently from the mesh. The results obtained show that the dimensionless SIFs for the pure modes I and II increase with increase in the crack length but the angle in which pure mode-II occurs decreases. For the mixed-mode loading, with increase in the crack angle, N_I value decreases, while N_{II} value increases to a maximum value and then decreases. The results obtained from the crack propagation examinations show that the crack angle has an important effect on the crack initiation angle. The crack initiation angle increases with increase in the crack angle. When the crack angle is zero, then the crack is propagated along its initial direction, whereas in the mixed-mode cases, the crack deviates from the initial direction, and propagates in a direction (approximately) parallel to the direction of maximum compressive load.

Keywords: Cracked Brazilian Disc (CBD), Stress Intensity Factor (SIF), Extended Finite Element Method (X-FEM), Mixed-Mode.

1. Introduction

Discontinuities always exist in a rock medium. Most rock failures occur due to the stress concentration on the crack-tips and their propagations. Two principal subjects involved in the rock fracture are toughness and mode of the fracture. Fracture toughness is the critical value for the stress intensity factor (SIF) on the crack-tip. When SIF exceeds this value, the crack grows, and the direction of crack propagation also depends upon the loading condition and crack geometry. Generally, in a rock medium, crack occurs in pure mode-I, pure mode-II or mixed-mode I-II loading. In recent years, several laboratory specimens have been introduced to study fracturing in rocks. The cracked Brazilian disc (CBD) specimen, due to its simple geometry, easy preparation, and straight testing and loading condition, is widely used [1-5]. Also this specimen can be used in the determination of the mode-I, mode-II, and mixed-mode I-II fracture

toughness. Determination of fracture toughness in this specimen requires calculating the stress intensity factor (SIF) on the crack-tip; one way for this calculation is using the finite element method (FEM). In this method, the discontinuity must be located on the boundary of elements, and this method also requires implementing a special mesh generation on the crack-tip, so that it can be used to calculate SIF. These problems have led to the development of a new method named extended-finite element method (X-FEM). In this method, discontinuous enrichment functions are added to the finite element approximation to account for the presence of the crack. Hence, the discontinuity is independent from the mesh, and, unlike FEM, there is no need to re-mesh the domain in the crack growth process. In X-FEM, an initial discretization is generated, and then different crack geometries are inserted into it. X-FEM was first proposed by Belytschko and Black [6]. They

provided a method based on FEM to model crack growth by minimizing re-meshing. Moës et al. [7] improved this method, so that the entire crack domain is modeled completely independent from the mesh. They called this X-FEM. However, the most significant and effective step in developing X-FEM was achieved by Dolbow [8].

Considering the importance of crack-tip SIF calculation and X-FEM efficiency in problems involving crack, this study was aimed to calculate SIF on crack-tip and also crack propagation direction in the CBD specimen for various geometrical crack conditions (i.e. different crack length and different angles with respect to the diametrical loading) using X-FEM. An object-oriented code called MEX-FEM, based on X-FEM, was developed to simulate the crack in the rock medium. In this code, SIF in the crack-tip is calculated through the interaction integral, and the crack growth direction is predicted using the maximum tangential stress criterion.

The outline of this work is as follows. Description of the CBD model is presented in Section 2. Section 3 is devoted to the brief definition of the X-FEM approximations for the problems in the linear elastic fracture mechanics. Determination of SIF in the CBD specimens is presented in Section 4. Section 5 presents the conclusion of this work.

2. Cracked Brazilian Disc (CBD) specimen

The CBD specimen has been initially used by Awaji and Sato [9]. The geometry of the CBD specimen is shown in Figure 1. Atkinson et al. [10] have formulated SIF for this model geometry. This method allows testing under mode-I, mode-II and mixed-mode I-II loading conditions using the same specimen arrangement and experimental set-up.

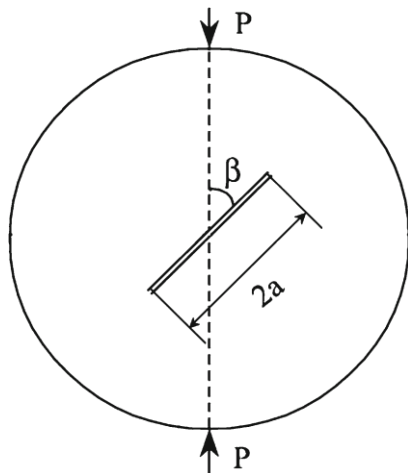


Figure 1. Geometry of CBD specimen.

The expressions below are used for the fracture toughness computation of CBD:

$$K_I = \frac{P\sqrt{a}}{\sqrt{\pi RB}} N_I \tag{1}$$

$$K_{II} = \frac{P\sqrt{a}}{\sqrt{\pi RB}} N_{II} \tag{2}$$

where K_I is mode-I stress intensity factor, K_{II} is mode-II stress intensity factor, R is the radius of CBD, B is the thickness of the disk, P is the compressive load at failure, a is the half-crack length, and N_I and N_{II} values are the dimensionless stress intensity factors that depend on the ratio of half crack to radius (a/R) and crack orientation angles with respect to the diametrical load [4].

Atkinson, et al. [10] have considered two- and five-term approximations, and also a simplified short crack approximation in order to determine SIF in the CBD specimen. Although there is a difference between the results obtained for these approximations, their comparison has shown that the approximate of the short crack for a crack length (a/R) smaller than 0.3 has an acceptable accuracy. Also the results obtained show that the two- and five-term approximations have very close results. The following equations have been proposed to approximate SIFs [10]:

$$N_I = T_1(1 - 4\sin^2(\beta)) + T_2(8\sin^2(\beta)(1 - 4\cos^2(\beta)))\left(\frac{a}{R}\right)^2 \tag{3}$$

$$N_{II} = 2\sin(2\beta)[S_1 + S_2(8\cos^2(\beta) - 5)\left(\frac{a}{R}\right)^2] \tag{4}$$

where T_i and S_i are the numerical factors, with their values given in Table 1.

Table 1. T_i and S_i values for equations (3) and (4).

(a/R)	T_1	T_2	S_1	S_2
0.1	1.014998	0.503597	1.009987	0.502341
0.2	1.060049	0.514907	1.039864	0.509959
0.3	1.135551	0.533477	1.089702	0.522272
0.4	1.243134	0.559734	1.160796	0.539824
0.5	1.387239	0.594892	1.257488	0.563966
0.6	1.578258	0.642124	1.390654	0.597985

3. Extended-finite element method (X-FEM)

This method is based upon the finite element and partition of unity methods. The idea is to enrich the usual finite element spaces with additional degrees of freedom to account for the presence of the crack [11]. Since the mesh does not need to conform to the problem geometry, there is no need for re-meshing during the crack propagation. Existence of the crack causes two different enrichment types in the problem: crack interior and crack tip enrichments. The nodes whose nodal shape function support intersects the interior of

the crack are enriched by a step function, and the element nodes that contain the crack-tip are enriched by the 2D linear elastic asymptotic near-tip fields (as seen in Figure 2) [12]. The interior of a crack is modeled by the generalized Heaviside enrichment function H , where H takes on the value +1 above the crack and -1 below the crack:

$$H(x) = \begin{cases} +1 & \text{for } x > 0 \\ -1 & \text{for } x < 0 \end{cases} \quad (5)$$

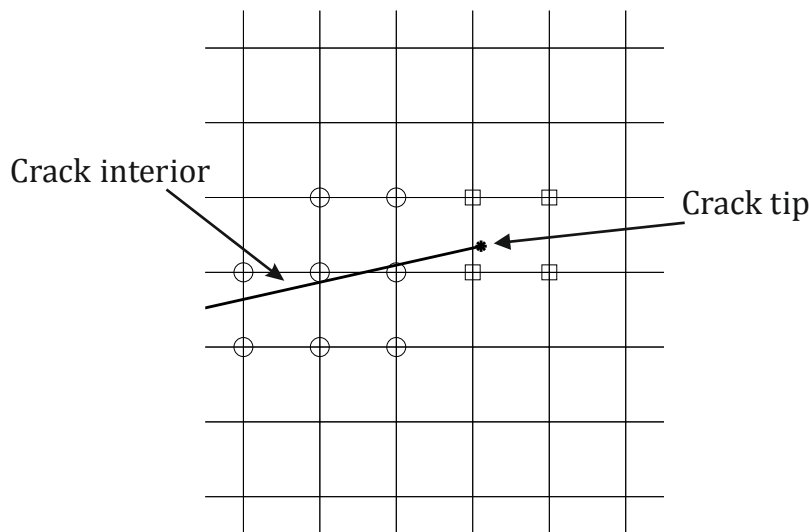


Figure 2. Illustration of a crack on a mesh. Circled nodes are enriched by Heaviside function, and squared nodes are enriched by near-tip functions.

In order to model the crack-tip, and also to improve the representation of crack-tip fields, crack-tip enrichment functions were used. For an isotropic material, the crack-tip enrichment functions are given as [13]:

$$\{F_j(r, \theta)\}_{j=1,2,3,4} = \left\{ \begin{array}{l} \sqrt{r} \sin \frac{\theta}{2}, \sqrt{r} \cos \frac{\theta}{2}, \\ \sqrt{r} \sin \frac{\theta}{2} \sin \theta, \sqrt{r} \cos \frac{\theta}{2} \sin \theta \end{array} \right\} \quad (6)$$

Among these functions, only the first one is discontinuous, indicating that discontinuity of the function is along the two faces of the crack. The extended finite element approximation for the displacement field is [12]:

$$u^h(x) = \sum_{i \in I} N_i(x) u_i + \sum_{j \in J} N_j(x) H_j(x) a_j + \sum_{k \in K} N_k(x) \sum_{l=1}^4 F_l(x) b_k^l \quad (7)$$

where $N(x)$ is a shape function, u_i is a nodal displacement (standard degree of freedom), a_j is a

vector of additional degree for the nodal freedom associated with the Heaviside function, and b_k^l is a vector of additional degree for the nodal associated with the elastic asymptotic crack-tip functions. In the above equation, I is the set of all nodes in the mesh, J is the set of nodes enriched with discontinuous enrichment, and K is the set of nodes enriched with asymptotic enrichment. Stress intensity factors are computed using the domain forms of the interaction integrals [12]:

$$I^{(1,2)} = \int_A [\sigma_{ij}^{(1)} \frac{\partial u_i^{(2)}}{\partial x_1} + \sigma_{ij}^{(2)} \frac{\partial u_i^{(1)}}{\partial x_1} - w^{(1,2)} \delta_{1j}] \frac{\partial q}{\partial x_j} dA \quad (8)$$

This integral is calculated over the elements intersected by a circle of radius r_d , and centered at crack-tip (i.e. the shaded elements in Figure 3). The relationship between stress intensity factors and interaction integral is [12]:

$$I^{(1,2)} = \frac{2}{E'} (K_I^{(1)} K_I^{(2)} + K_{II}^{(1)} K_{II}^{(2)}) \quad (9)$$

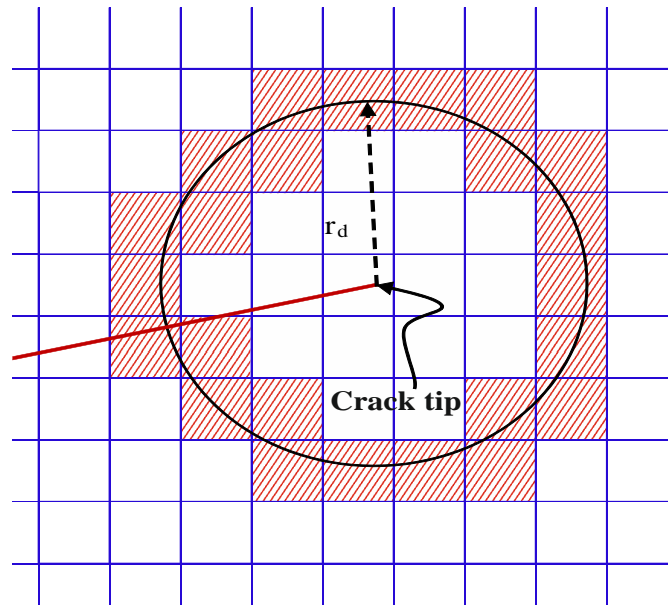


Figure 3. Illustration of elements for calculation of interaction integral (shaded elements).

Prediction of the crack growth direction is one of the important problems involved in the fracture mechanics. Although several different criteria have been proposed for determining the direction of crack propagation under general mixed-mode loading conditions, the most commonly used ones are the maximum tangential stress (MTS) criterion [14], the maximum energy release rate criterion [15], and also the minimum strain energy density [16]. However, the maximum tangential stress criterion in which the crack is propagated from crack-tip along the direction of maximum tangential stress has been used more extensively in X-FEM for modeling crack growth. Therefore, this criterion was used for determining the crack growth direction in this study. The direction of crack growth is calculated using the following equation:

$$\theta_c = 2 \tan^{-1} \frac{1}{4} \left(\frac{K_I}{K_{II}} \pm \sqrt{\left(\frac{K_I}{K_{II}} \right)^2 + 8} \right) \quad (10)$$

where θ_c is the crack growth angle, and K_I and K_{II} are stress intensity factor modes I and II, respectively.

4. SIF in CBD specimen

As mentioned earlier, in X-FEM, an initial discretization is generated, and then different crack geometries can be considered into it. When

the crack angle from the loading axis is zero, pure mode-I occurs. Variation in the dimensionless stress intensity factor for pure mode-I (N_I) with crack length ratio (a/R) is shown in Figure 4. N_I value for pure mode-I increases with increase in the crack length. Changing the crack angle produces different combinations of modes I and II. Figure 5 shows the results obtained from this study for $a/R = 0.1$, and the results given by Atkinson, et al. [10]. As it can be seen in this figure, the values obtained using X-FEM are in good agreement with the results obtained by Atkinson et al. [10].

Variations in the N_I and N_{II} values with the crack angles for different crack length ratios are shown in Figure 6. With increase in the crack angle, N_I value decreases but N_{II} value increases to a maximum one and then decreases. Theoretically, pure mode-II occurs when N_I value is zero for a mixed-mode loading condition. For different crack lengths, pure mode-II occurs at different angles. These angles can be obtained from Figure 6. The pure mode-II angles for various crack lengths are shown in Figure 7. Note that the angle for pure mode-II decreases with increase in the crack length. Figure 8 shows the variation in the N_{II} values for pure mode-II with the crack length ratio. N_{II} value for pure mode-II increases with increase in the crack length.

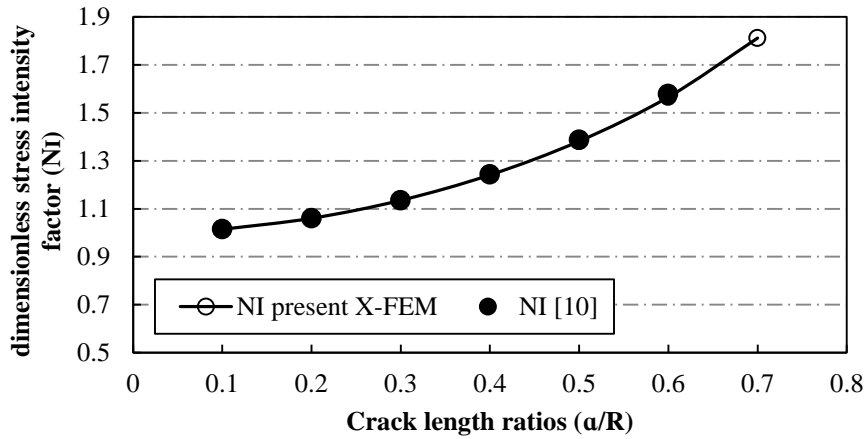


Figure 4. Variation in N_I values with crack length ratios.

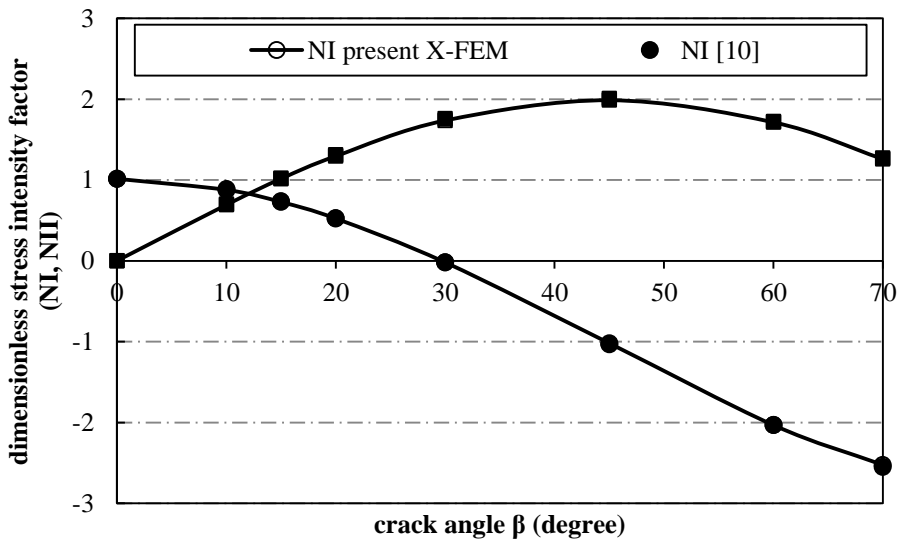


Figure 5. Variations in N_I and N_{II} values with crack angle β .

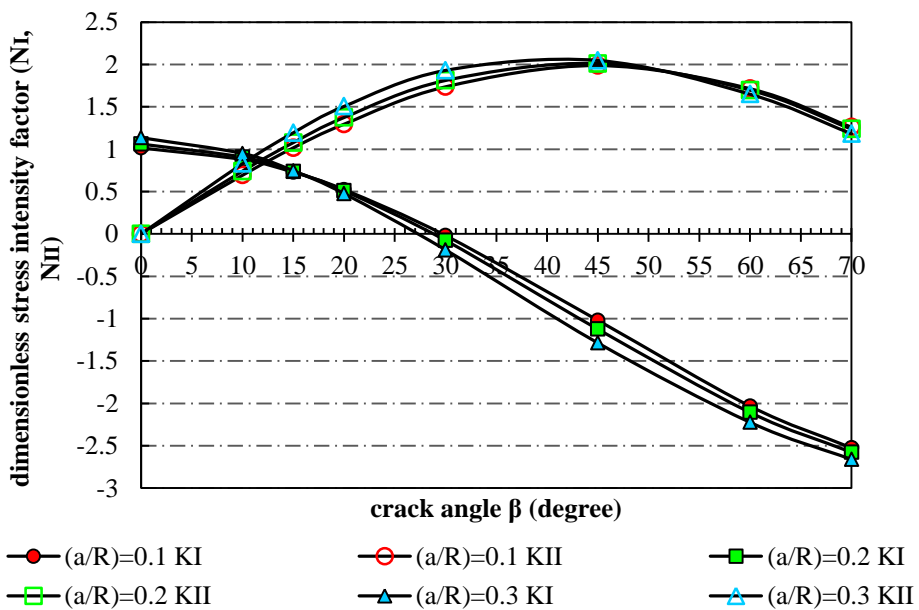


Figure 6a. Variations in N_I and N_{II} values with crack angle β : a) (a/R)=0.1-0.3; b) (a/R)=0.4-0.7.

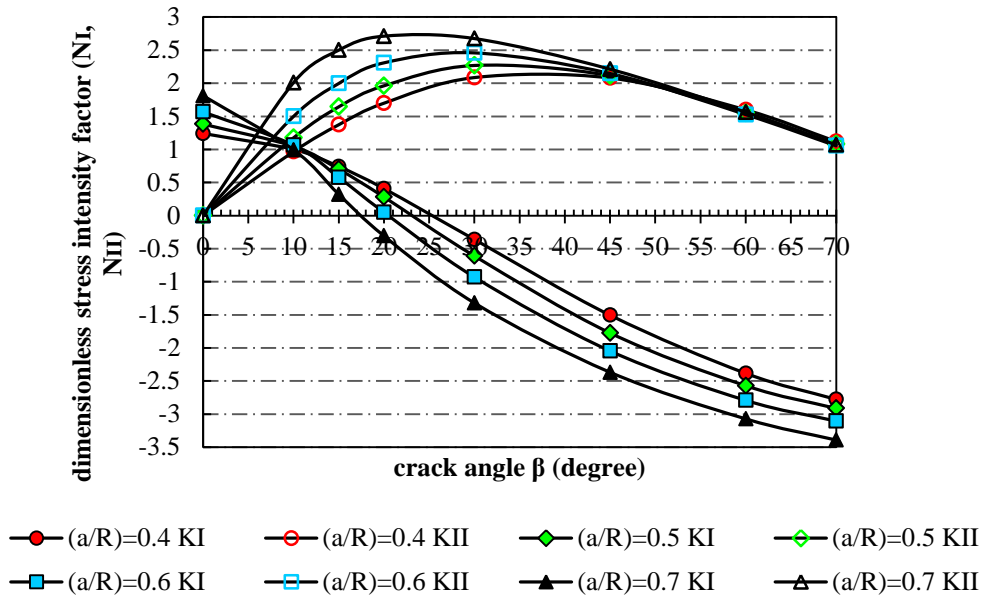


Figure 6b. Variations in N_I and N_{II} values with crack angle β : a) $(a/R)=0.1-0.3$; b) $(a/R)=0.4-0.7$.

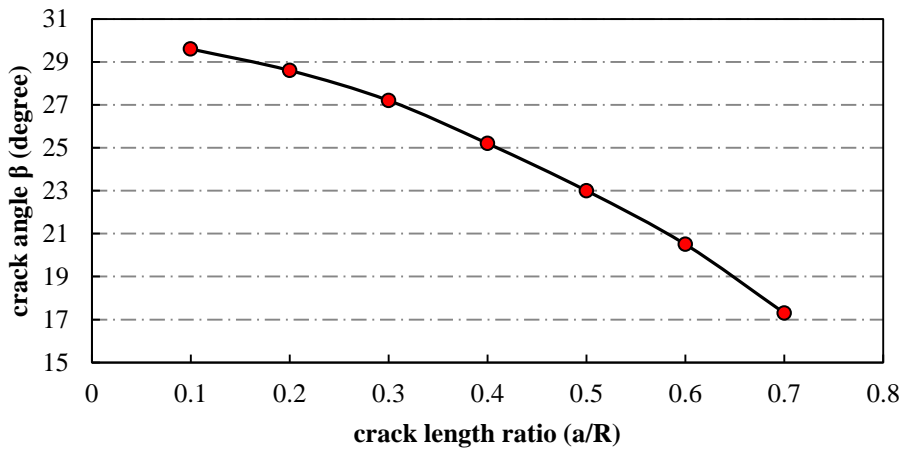


Figure 7. Variation in crack angle of pure mode-II with (a/R) .

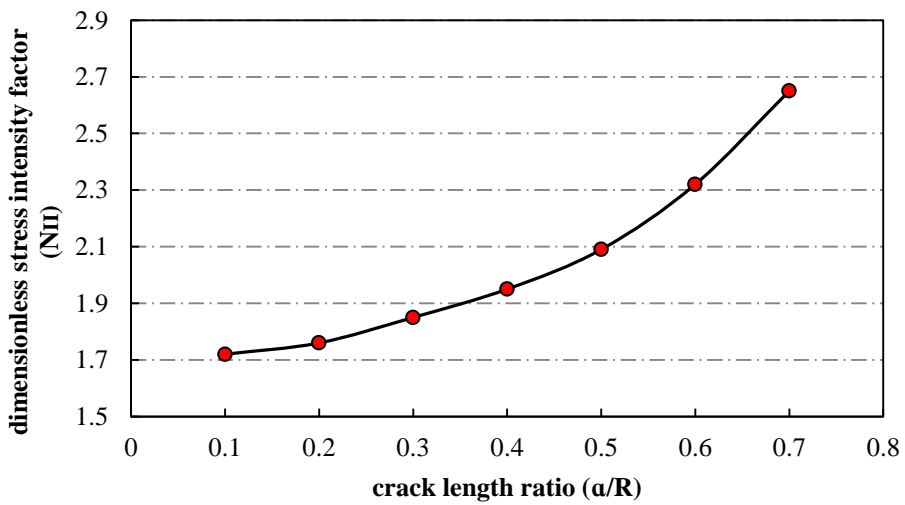


Figure 8. Variation in N_{II} value with crack length ratio.

5. Crack propagation in CBD specimen

In this work, quasi-static crack propagation in the CBD specimen was simulated using MEX-FEM. In the simulation, the crack propagation angle, θ_c , was determined using the maximum tangential stress criterion. The crack modeling in X-FEM is mesh-independent, i.e. the finite element mesh is generated before the analysis starts. In order to make the results applicable to more practical conditions, the analysis was conducted only for those values of α having $K_I \geq 0$.

The result obtained for the crack propagation examinations show that for the crack angle of zero, pure mode-I occurs, and thus the crack

initiation angle equals zero. In the other cases and under the mixed-mode conditions, the crack angle has an important effect on the crack initiation angle. As for the increase in the crack angle, the crack initiation angle increases as well, as shown in Figure 9.

As shown in this figure, the effect of crack length on the crack initiation angle is smaller in comparison to the effect of the crack angle on it. As in the crack lengths (a/R) of 0.1 and 0.2, there is no significant difference in the magnitude of crack initiation angle. The effect is more obvious for the increase in the crack length.

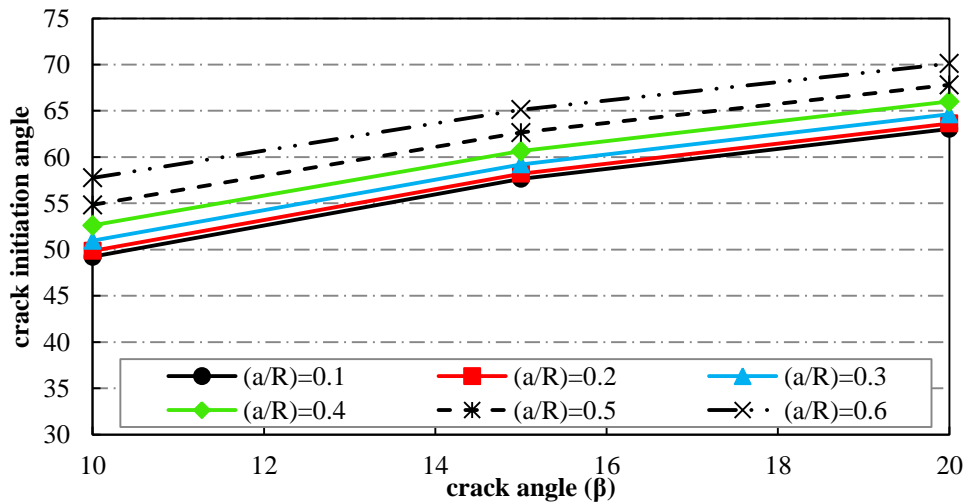


Figure 9. Variation in crack initiation angle with crack angle.

The CBD specimens were simulated by MEX-FEM, and the crack propagation paths in the specimen with crack length ratio of 0.3 and crack angles of 0, 10, and 20 were shown in Figure 10. It can be seen that when the crack angle is zero (as shown in Figure 10a), the specimen is subjected to pure mode-I and the crack grows along its primary

angle, whereas, in the combinational cases, it deviates from the initial direction, and propagates toward the loading points. Therefore, as reported in the literature [17], the crack inclination angle in rock-like specimens has a significant effect on their final breakage.

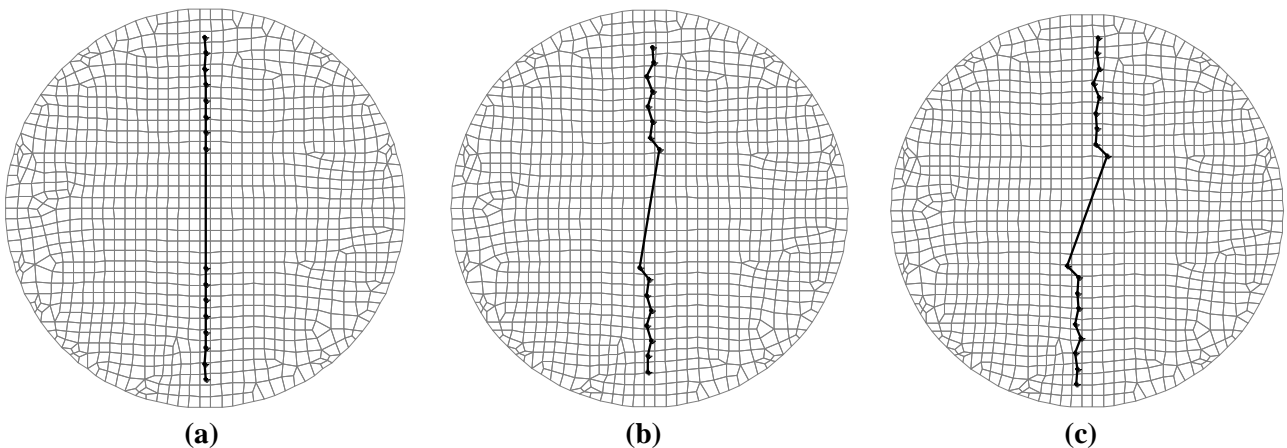


Figure 10. Crack propagation path in CBD specimens with different crack inclination angles: a) $\beta=0^\circ$; b) $\beta=10^\circ$; c) $\beta=20^\circ$.

6. Conclusions

In this work, the extended finite element method (X-FEM) was used to evaluate the stress intensity factor (SIF) for various crack geometries in the CBD specimen. This method is based upon the finite element method (FEM), and employs the enrichment functions for crack modeling independent from the element. Different crack geometries can be easily inserted in a similar discretization. These results coincide with the previous results reported in the literature. The results show that with increase in the crack length, the dimensionless stress intensity factors for pure modes I and II increase, while the angle for pure mode-II decreases. For mixed-mode loading, N_I value decreases with increase in the crack angle, whereas N_{II} value increases to a maximum and then decreases. Furthermore, the results obtained for the crack propagation examinations show that the crack angle has an important effect on the crack initiation angle. The crack initiation angle increases with increase in the crack angle. When the crack angle is zero, the crack grows along its initial direction, whereas, in the mixed-mode cases, the crack deviates from the initial direction, and propagates toward the loading points. Therefore, the crack inclination angle in rock-like specimens has a significant effect on their final breakage. The results obtained from this work also demonstrate the X-FEM potential to simulate the crack in rock materials.

References

[1]. Ayatollahi, M. and Aliha, M. (2005). Cracked Brazilian disc specimen subjected to mode II deformation, *Engineering fracture mechanics*. 72 (4): 493- 503.

[2]. Ayatollahi, M. and Aliha, M. (2008). On the use of Brazilian disc specimen for calculating mixed mode I–II fracture toughness of rock materials, *Engineering Fracture Mechanics*. 75 (16): 4631- 4641.

[3]. Ayatollahi, M. and Sistaninia, M. (2011). Mode II fracture study of rocks using Brazilian disk specimens, *International Journal of Rock Mechanics and Mining Sciences*. 48 (5): 819- 826.

[4]. Ghazvinian, A., Nejati, H. R., Sarfarazi, V. and Hadei, M. R. (2013). Mixed mode crack propagation in low brittle rock-like materials, *Arabian Journal of Geosciences*. 6 (11): 4435- 4444.

[5]. Markides, C. F., Pazis, D. and Kourkoulis, S. (2013). The centrally cracked Brazilian disc: closed solutions for stresses and displacements for cracks

under opening mode, *Journal of Engineering Mathematics*. 83 (1): 143- 168.

[6]. Belytschko, T. and Black, T. (1999). Elastic crack growth in finite elements with minimal remeshing, *International journal for numerical methods in engineering*. 45 (5): 601- 620.

[7]. Moës, N., Dolbow, J. and Belytschko, T. (1999). A finite element method for crack growth without remeshing, *Int. J. Numer. Meth. Engng*. 46: 131- 150.

[8]. Dolbow, J. E. (1999). An extended finite element method with discontinuous enrichment for applied mechanics, *Northwestern university*.

[9]. Awaji, H. and Sato, S. (1978). Combined mode fracture toughness measurement by the disk test, *Journal of Engineering Materials and Technology*. 100: 175.

[10]. Atkinson, C., Smelser, R. and Sanchez, J. (1982). Combined mode fracture via the cracked Brazilian disk test, *International Journal of Fracture*, 18 (4): 279- 291.

[11]. Richardson, C. L., Hegemann, J., Sifakis, E., Hellrung, J. and Teran, J. M. (2011). An XFEM method for modeling geometrically elaborate crack propagation in brittle materials, *International Journal for Numerical Methods in Engineering*. 88 (10): 1042- 1065.

[12]. Sukumar, N. and Prévost, J. H. (2003). Modeling quasi-static crack growth with the extended finite element method Part I: Computer implementation, *International Journal of Solids and Structures*. 40 (26): 7513- 7537.

[13]. Fleming, M., Chu, Y., Moran, B., Belytschko, T., Lu, Y. and Gu, L. (1997). Enriched element-free Galerkin methods for crack tip fields, *International Journal for Numerical Methods in Engineering*. 40 (8): 1483- 1504.

[14]. Erdogan, F. and Sih, G. (1963). On the crack extension in plates under plane loading and transverse shear, *Journal of basic engineering*. 85: 519.

[15]. Nuismer, R. (1975). An energy release rate criterion for mixed mode fracture, *International Journal of Fracture*. 11 (2): 245- 250.

[16]. Sih, G. C. (1974). Strain-energy-density factor applied to mixed mode crack problems, *International Journal of Fracture*. 10 (3): 305- 321.

[17]. Haeri, H., Shahrari, K., Marji, M. F. and Moarefvand, P. (2014). Experimental and numerical study of crack propagation and coalescence in pre-cracked rock-like disks, *International Journal of Rock Mechanics and Mining Sciences*. 67: 20- 28.

شبیه‌سازی گسترش ترک در نمونه دیسک برزلی ترک‌دار با استفاده از المان محدود توسعه‌یافته

مصلح افتخاری*، علیرضا باغبانان و حمید هاشم‌الحسینی

دانشکده مهندسی معدن، دانشگاه صنعتی اصفهان، ایران

ارسال ۲۰۱۴/۵/۱۹، پذیرش ۲۰۱۵/۲/۲۲

* نویسنده مسئول مکاتبات: eftekhari_mosleh@yahoo.com

چکیده:

نمونه دیسک برزلی ترک‌دار به‌طور گسترده‌ای به‌منظور تعیین چقرمگی مودهای خالص یک و دو و همچنین مود ترکیبی استفاده می‌شود. در این تحقیق، فاکتور شدت تنش نوک ترک و همچنین مسیر گسترش ترک در این نمونه برای شرایط مختلف ترک با استفاده از روش المان محدود توسعه‌یافته محاسبه می‌شود. روش المان محدود توسعه‌یافته مبتنی بر روش المان محدود است و در آن ترک مستقل از شبکه‌بندی مدل‌سازی می‌شود. نتایج نشان می‌دهد که فاکتور شدت تنش بدون بعد برای مودهای خالص یک و دو با افزایش طول ترک افزایش می‌یابد در حالی که زاویه‌ای که در آن مود خالص دو رخ می‌دهد، کاهش می‌یابد. برای حالت بارگذاری مود ترکیبی با افزایش طول ترک، مقدار N_I کاهش می‌یابد اما مقدار N_{II} تا یک مقدار حداکثری افزایش و پس از آن کاهش می‌یابد. نتایج بررسی‌های گسترش ترک در این نمونه‌ها نشان می‌دهد که زاویه ترک نقش مهمی در میزان زاویه شروع ترک دارد به‌طوری‌که با افزایش زاویه ترک، زاویه شروع ترک افزایش می‌یابد. زمانی که زاویه ترک صفر باشد ترک در جهت اولیه خود گسترش می‌یابد در حالی که در موارد مود ترکیبی، ترک از مسیر خود منحرف‌شده و به سمت محل بارگذاری گسترش می‌یابد.

کلمات کلیدی: دیسک برزلی ترک‌دار، فاکتور شدت تنش، روش المان محدود توسعه‌یافته، مود ترکیبی.
